Centrum voor Wiskunde en Informatica
REPORT*RAPPORT*

A Mathematical Model for Preflush Treatment in an Oil Reservoir Using a Fully Miscible Fluid

F.J. Vermolen, G. Pieters, J. Bruining, P.L.J. Zitha

Modelling, Analysis and Simulation (MAS)

MAS-R9929 September 30, 1999

Report MAS-R9929
ISSN 1386-3703

CWI
P.O. Box 94079
1090 GB Amsterdam
The Netherlands

A Mathematical Model for Preflush Treatment in an Oil Reservoir Using a Fully Miscible Fluid

Fred Vermolen
CWI
P.O.Box 94079, 1090 GB Amsterdam, The Netherlands

Gert-Jan Pieters
Faculty of Technical Mathematics and Informatics
Delft University of Technology
P.O. Box 5031, 2600 GA Delft, The Netherlands

Pacelli Zitha, Hans Bruining
Faculty of Applied Earth Sciences
Delft University of Technology
Mijnbouwstraat 120, 2628 RX Delft, The Netherlands

ABSTRACT

In this paper we propose and analyse a mathematical model for preflush treatment in an oil reservoir. The model is based on two phase flow in which both phases are fully miscible. For the case of constant injection rate condition, fully implicit solutions can be constructed. Saturation profiles consist of shocks and fingering zones. For constant pressure conditions we construct a semi-explicit relation for the shock position and the gel penetration depth. The model predicts diversion behaviour of polymer-gel treatment from low permeability layers and hence viscous preflush improves the efficiency of polymer-gel treatment.

1991 Mathematics Subject Classification: 35R35, 76S05
Keywords and Phrases: hyperbolic equations, travelling wave, gel treatment, preflush treatment, porous media
Note: Research funded by the European Union (Welgel project).

1. Introduction

Polymer gels are used in a widely variety of fields including improved oil and gas recovery, confinement of ground water contaminants, water treatment plant growth control and filtration to mention only a few. Of special interest to us is the application of polymer gels to reduce water production during oil and gas recovery, which is representative of a larger class of situations involving polymer gels in porous media. Mature oil fields suffer from excessive water production. Large water production creates serious environmental problems concerning water waste disposal. Additionally operation cost increase and large oil reserves remain unproduced. A major cause for this is water-chanelling through high permeability layers in reservoirs.

To minimise water production, polymers and crosslinkers in aqueous solution are injected in the near-wellbore region, aiming at decreasing water relative permeability, while maintaining oil relative permeability. Polymers react with crosslinkers and then form a gel (gelation). The gel adsorps on the skeleton of the porous medium in the reservoir and consequently the (relative) permeability of water decreases. Due to high temperatures usually present in reservoirs, gelation is often rapid. Thus the gel can be formed prematurely and its penetration depth may be smaller than the desired value. This would result in an inefficient gel treatment. Another reason for a poor efficiency of gel treatments can be precipitation of crosslinkers, which results in a weaker gel.
To delay gelation and to prevent precipitation of crosslinkers a cold, acetatic preflush treatment is carried out on the reservoir prior to gel treatment aiming at a delay (control) of gelation and an increase of the acidity. The injected preflush consists of a fluid with a high viscosity and is fully miscible with water. An other aim of a viscous preflush treatment is minimization of gel penetration in low permeability layers. Viscous preflush then increases the efficiency of the gel treatment. It is our aim to analyse a simplified model for this preflush treatment.
The remaining paper is organised in four sections. Section 2 deals with the formulation of the model. Section 3 gives an explicit solution both for cases of one and multiple layers. Section 4 gives a comparison of the analytical and numerical solutions. In Section 5 we end with some conclusions.

2. Model

In this section we formulate a model for flow of two miscible phases in porous media. We consider a radially symmetric reservoir of constant thickness, H (m). At the central axis a well with radius r_w (m) is present which extends over the whole thickness of the reservoir. Initially the reservoir is saturated with water. At $t = 0$, t (s) denotes time, injection of a viscous preflush phases is started through the well into the reservoir. Injection of viscous phases takes place during $t \in (0, T)$. For $t > T$ water with polymer is injected again. Initially the preflush phase is absent in the reservoir. We assume that the presence of polymer in water solution hardly affects the water viscosity. Polymer pore wall interactions are disregarded. Polymer is assumed to be Newtonian and flow is incompressible.

2.1 Transport

Let the porous medium be homogeneous and isotropic with porosity ϕ. Assuming the flow to be uniformly distributed across the thickness of the reservoir, the specific discharge of each phase (q_i in m/s) is given by:

$$q_i = \frac{Q_i}{2\pi r_w H}, \quad i \in \{1, 2\},$$

where indices $i = 1$ and $i = 2$ respectively correspond to the viscous phase and to water. Furthermore Q_i (m^3/s) represents the volumetric flow of phase i into the reservoir.

2.2 Equations

Here we formulate mass balance equations for the viscous phase and water in the reservoir. Since injected saturations of both phases are constant over the height of the reservoir and gravity can be disregarded, all saturations are functions of the horizontal distance r (m) and time t (s) only. Consequently the mass balance equations for $r > r_w$ and $t > 0$ are given by

$$\phi \frac{\partial S_i}{\partial t} + \frac{1}{r}\frac{\partial}{\partial r}\left(r\, q_i\right) = 0, \quad i \in \{1, 2\}. \tag{2.1}$$

Here S_i $(-)$ denotes the saturation of phase i. Saturations satisfy $S_1 + S_2 = 1$. The specific discharge, q_i (m/s), is related to the pressure, p (Pa), via Darcy's Law, i.e. for $r > r_w$ and $t > 0$

$$q_i = -\frac{k_0\, k_{ri}}{\mu_i}\frac{\partial p}{\partial r}, \quad i \in \{1, 2\}. \tag{2.2}$$

Here k_0 (m^2), μ_i $(Pa\, s)$ and k_{ri} respectively denote the permeability of the porous medium, the viscosity of phase i and the relative permeability of phase i $(\mu_1 > \mu_2)$. Since the phases are miscible, capillary pressure is zero. The relative permeability is a function of the saturation, i.e.

$$k_{ri} = k_{ri}(S_i).$$

Summation of equation (2.1) over $i \in \{1, 2\}$, using $S_1 + S_2 = 1$ and subsequent integration yields for $r > r_w$ and $t > 0$

$$r \cdot (q_1 + q_2) = Q(t),$$

where $Q(t)$ (m^2/s) is a positive integrable function of time t. Combination of equation (2.2) with above relation yields for all $r > r_w$ and $t > 0$

$$q_1 = \frac{Q(t)}{r \cdot \left(1 + \frac{k_{r2}\mu_1}{k_{r1}\mu_2}\right)} =: \frac{Q(t)}{r}\, f(S_1), \tag{2.3}$$

where $f(S_1)$ represents the flux-function. Equation (2.3) allows us to write for all $r > r_w$, $t > 0$

$$\phi \frac{\partial S_1}{\partial t} + \frac{Q(t)}{r}\frac{\partial f(S_1)}{\partial r} = 0. \tag{2.4}$$

Introducing the co-ordinate transformation $x = \dfrac{\phi(r^2 - r_w^2)}{2}$ and substitution this into equation (2.4) gives:

$$\frac{\partial S_1}{\partial t} + Q(t)\frac{\partial f(S_1)}{\partial x} = 0, \quad \text{for all} \quad x > 0,\ t > 0. \tag{2.5}$$

In the x,t-space $Q(t)$ is interpreted as a velocity. Initially the porous medium is saturated with water, hence $S_2 = 1$ and $S_1 = 0$ at $t = 0$. Between $t = 0$ and $t = T$ the viscous preflush phase is injected, i.e. $S_1 = 1$ at $x = 0$ for $0 < t \leq T$. After $t = T$ water is injected again, i.e. $S_1 = 0$ at $x = 0$ for $t \geq T$. Hence as initial and boundary conditions we have (IB)

$$(IB) \quad \begin{cases} S_1(x,0) = 0, \quad x > 0 \\ \\ S_1(0,t) = \begin{cases} 1, & 0 < t < T \\ 0, & t \geq T. \end{cases} \end{cases}$$

In Section 3 equation (2.5) with initial and boundary conditions (IB) is subject to analysis. We give a fully implicit solution for the fully miscible case, i.e. [1]

$$k_{ri}(S_i) = S_i, \quad S_i \in [0,1], \quad i \in \{0,1\}. \tag{2.6}$$

For more general cases where capillarity effects are neglected, semi-explicit solutions using the method of characteristics can be obtained.

In the present work we consider two classes of boundary conditions:

- constant injection rate condition: Q_i is taken constant at any time, and hence the pressure drop over the injection point and its surroundings is allowed to change in time;
- constant pressure condition: Δp is taken constant in time and hence the injection rate is allowed to change in time.

3. Analysis

In this section we deal with the case of two fully miscible phases, see equation (2.6). The flux-function then becomes

$$f(S_1) = \frac{S_1}{S_1 + (1 - S_1)\frac{\mu_1}{\mu_2}}, \text{ with } E := \frac{\mu_1}{\mu_2}. \tag{3.1}$$

Since $\mu_1 > \mu_2$ it can be shown using equation (3.1) that $f''(S_1) > 0$ for all $0 \leq S_1 \leq 1$. On the contrary if $\mu_1 < \mu_2$ then $f''(S_1) < 0$ for all $0 \leq S_1 \leq 1$. Note that if $\mu_1 = \mu_2$ then $f(S_1) = S_1$ and this case corresponds to single phase flow. Since for $0 < t < T$ we inject $S_1 = 1$, it is clear from the entropy condition [7] that the interface between the viscous phase and water is a stable shock. This is illustrated in Figure 1 by a sketch of characteristics in the x,t-plane, where characteristics originating from the x and t-axis (for $0 < t < T$) intersect. This shock, at position $s(t)$, travels with velocity

$$\dot{s}(t) = \frac{f(S_1(s_+(t),t)) - f(S_1(s_-(t),t))}{S_1(s_+(t),t) - S_1(s_-(t),t)} = \frac{1}{S_1(s_-(t),t) + (1 - S_1(s_-(t),t)) \cdot E}. \tag{3.2}$$

In Figure 1 it can be seen that there exists a $\tau \geq T$ such that $\dot{s}(t) = Q(t)$ (hence $s(t) = \int_0^t Q(s)ds$) for all $0 < t \leq \tau$ and $0 < \dot{s}(t) < Q(t)$ for all $t > \tau$. This τ is indicated in Figure 1.

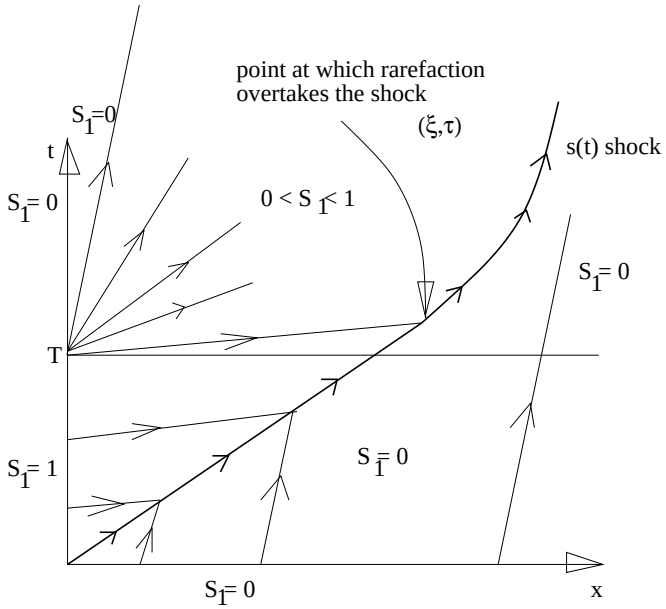

Figure 1: Sketch of characteristics in the x, t-plane.

For $t > T$ the boundary condition is changed and from the entropy condition [7] a rarefaction between water and the viscous phases results (see Figure 1), whereas the shock between the viscous phase and water, $s(t)$, continues to move. In the rarefaction part the saturation is continuous and we derive a self-similar solution. Both phases are fully miscible. However, due to absence of molecular diffusion, the phases do not actually mix on a microscale. Since equation 2.1 holds on an upscaled macro-scale, the continuous part of the solution is interpreted as a fingering zone [5], which is a mixing taking place on a pore scale. We seek solutions of the form

$$S_1(x,t) = \overline{S}_1(\eta), \quad \eta := \frac{x}{\int_T^t Q(\chi)d\chi}.$$

Substitution of this transformation into equation (2.5) gives

$$\overline{S}_1' = 0 \quad \text{or} \quad \eta = f'(S_1).$$

The first solution corresponds to a shock, which occurs at the interface between viscous phase and water. For cases in which k_{ri} is a complicated function of S_1, we are not able to solve above equation explicitly. The second solution represents a rarefaction (fingering) part between water and the viscous phase. Assuming that both phases are fully miscible, we combine equations (2.3) and (2.6) with above relation to obtain

$$\overline{S}_1(\eta) = \frac{\sqrt{\frac{E}{\eta}} - E}{1 - E}. \tag{3.3}$$

Above relation holds for the rarefaction part of the saturation profile, i.e. $\overline{S}_1(\eta)$ is continuous for a region $\eta_L < \eta < \eta_R$. We are interested in solutions $\overline{S}_1(\eta) \in [0,1]$, see (IB). From above relation follows that $\overline{S}(\eta)$ increases strictly monotonously since $\mu_1 > \mu_2$. Therefore there exists a pair (η_L, η_R) such that $\overline{S}_1(\eta_L) = 0$ and $\overline{S}_1(\eta_R) = 1$. Using above relation (η_L, η_R) are given by

$$\eta_L = \frac{1}{E} = \frac{\mu_2}{\mu_1} < 1, \quad \eta_R = E = \frac{\mu_1}{\mu_2} > 1,$$

note that $\mu_1 > \mu_2$. We introduce the positions $x_L(t)$ and $x_R(t)$ such that respectively $S_1(x_L(t), t) = 0$ and $S_2(x_R(t), t) = 1$ for all $T < t < \tau$. Since $\dfrac{\mu_1}{\mu_2} > 1$, it is clear that

$$\dot{x}_L(t) = \frac{1}{E}\, Q(t) < Q(t) = \dot{s}(t) < E\, Q(t) = \dot{x}_R(t).$$

Note that $x_L(t), \quad \forall t > T$ gives the maximal distance from the center of the well where we have the pure mixture of gel and water. This position will be referred to as the gel penetration depth. Since $Q(t) > 0$ and $Q(t)$ is integrable, from above relation follows that there exists a τ such that $x_R(\tau) = s(\tau)$. This time τ is the time at which the rarefaction (fingering) zone overtakes the shock. To find the time τ we need to solve problem (P):

$$\text{(P): Find } \tau \text{ such that } E \int_T^\tau Q(\chi)d\chi = \int_0^\tau Q(\chi)d\chi$$

$$\text{when Q is constant:} \quad \tau = \tfrac{\mu_1 T}{\mu_1 - \mu_2} > T.$$

For $t < \tau$ we have $s(t) = \int_0^t Q(\chi)d\chi$.

By combining the Rankine-Hugoniot condition (3.2), the solution (3.3) and $\eta = \frac{x}{\int_T^t Q(\chi)d\chi}$, one can derive the following ordinary differential equation for $s(t)$:

$$\dot{s}(t) = \sqrt{\frac{s(t)}{E \int_T^t Q(\chi)d\chi}}\, Q(t). \tag{3.4}$$

We require for physical reasons that the shock position $s(t)$ is a continuous function of time t. Then from continuity at $t = \tau$, it follows for the solution of (3.4):

$$s(t) = \left(\sqrt{s(\tau)} + \sqrt{\frac{1}{E}} \left\{ \left[\int_T^t Q(\chi)d\chi \right]^{\frac{1}{2}} - \left[\int_T^\tau Q(\chi)d\chi \right]^{\frac{1}{2}} \right\} \right)^2, \quad t > \tau. \tag{3.5}$$

Above relation causes the convex shape of the shock-curve, $s(t)$, for $t > T$ in the x,t-plane (see Figure 1). Using equation (3.3) and integrated expressions for $x_L(t)$, $x_R(t)$ we arrive

at the following expression which describes the saturation profile for all $x > 0$ and $t > 0$:

$$S_1(x,t) = \begin{cases} 0, \quad x \in \left[0, \left(\frac{1}{E}\int_T^t Q(\chi)d\chi\right)_+\right), \\ \\ \dfrac{\sqrt{\frac{E\int_T^t Q(\chi)d\chi}{x}} - E}{1-E}, \quad x \in \left[(\dfrac{1}{E}\displaystyle\int_T^t Q(\chi)d\chi)_+, \min\left\{s(t), E\displaystyle\int_T^t Q(\chi)d\chi\right\}\right), \\ \\ 1, \quad x \in \left[\left(E\int_T^t Q(\chi)d\chi\right)_+, s(t)\right), \quad t < \tau, \\ \\ 0, \quad x \geq s(t), \end{cases}$$

where the shock position $s(t)$ is given by

$$s(t) = \begin{cases} \int_0^t Q(\chi)d\chi, \quad t < \tau, \\ \\ \left(\sqrt{s(\tau)} + \sqrt{\dfrac{1}{E}}\left\{\left[\displaystyle\int_T^t Q(\chi)d\chi\right]^{\frac{1}{2}} - \left[\int_T^\tau Q(\chi)d\chi\right]^{\frac{1}{2}}\right\}\right)^2 \quad t \geq \tau. \end{cases}$$

The time τ is determined from problem (P). We see that $\dot{s}(t) = Q(t)$ for all $0 < t < T$ and $\dot{s}(t) \in (Q(t)/E, Q(t))$ for all $t > \tau$. Note that $s'(t) \to Q(t)/E$ as $t \to \infty$. Furthermore it is clear that the shock speed $\dot{s}(T)$ is not continuous for $t = \tau$.

3.1 Constant injection rate

For this case $Q(t) = Q$, hence above equations change into

$$S_1(x,t) = \begin{cases} 0, \quad x \in \left[0, \left(\frac{1}{E}Q(t-T)\right)_+\right), \\ \\ \dfrac{\sqrt{\frac{EQ(t-T)}{x}} - E}{1-E}, \quad x \in \left[(\dfrac{1}{E}Q(t-T))_+, \min\left\{s(t), EQ(t-T)\right\}\right), \\ \\ 1, \quad x \in \left[\left(EQ(t-T)\right)_+, s(t)\right), \quad t < \tau, \\ \\ 0, \quad x \geq s(t), \end{cases}$$

where the shock position $s(t)$ is given by

$$s(t) = \begin{cases} Qt, \quad t < \tau, \\ \\ \left(\sqrt{s(\tau)} + \sqrt{\dfrac{1}{E}Q}\left\{[(t-T)]^{\frac{1}{2}} - [(\tau - T]^{\frac{1}{2}}\right\}\right)^2 \quad t \geq \tau. \end{cases}$$

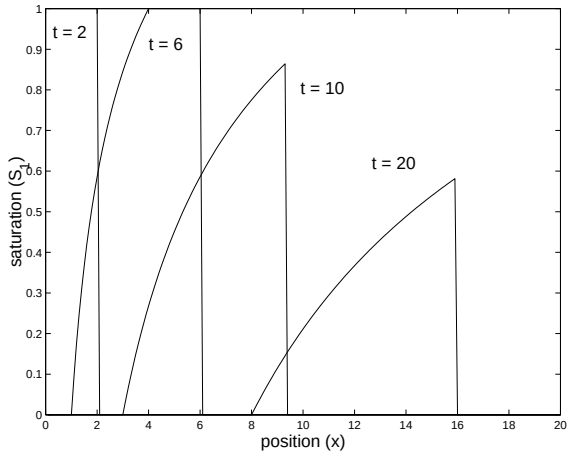

Figure 2: Saturation profiles at different times. Input data are mentioned in the text.

Here $\tau = \frac{\mu_1 T}{\mu_1 - \mu_2}$ and we note that the shock speed is not continuous at $t = \tau$. We give an example of the solution in Figure 2. Input parameters are $\mu_1 = 2$, $\mu_2 = 1$, $T = 4$. The curves correspond to times $t = 2, 4, 8$ and 10. In this example we set $Q(t) = 1$ at all times. It can be seen that the shock speed decreases with time for $t > \tau$ and that the profiles widen for $t > \tau$.

From integration of equation (2.2) we obtain for the pressure difference in cylindrical co-ordinates

$$\Delta p = -\frac{\mu_1 Q}{k_0} \cdot \int_{r_w}^{R} \frac{dr}{r\left(S_1(r,t)(1-E)+E\right)}, \quad t > 0, \tag{3.6}$$

where R (m) corresponds to the reservoir size and Δp (Pa) represents the pressure difference between the locations $r = r_w$ and $r = R$ (over the reservoir). Using co-ordinate transformation the pressure is computed from the solution in linear geometry by

$$\Delta p = -\frac{\mu_1 Q}{k_0 \phi} \cdot \int_{0}^{\frac{\phi(R^2 - r_w^2)}{2}} \frac{dx}{\left(r_w^2 + 2x/\phi\right)\left(S_1(x,t)(1-E)+E\right)}, \quad t > 0, \tag{3.7}$$

The integral in above equation can be evaluated explicitly using partial integration. It is decomposed in parts according to the expressions for the saturation profile.

3.2 Constant pressure condition

For the case that $\Delta p(t) = \Delta p$, one obtains for transformation of radial symmetry to linear geometry from equation (3.7) for $t > 0$

$$Q(t) = -\frac{k_0 \Delta p \phi}{\mu_1 I}, \quad I := \int_0^L \frac{dx}{\left(r_w^2 + 2x/\phi\right)\left(S_1(x,t)(1-E)+E\right)} \tag{3.8}$$

In above equation we defined $L := \frac{\phi(R^2 - r_w^2)}{2}$. Note that from above relation it follows that $I \neq I(t)$ (i.e. I is constant) for $E = 1$ $(\mu_1 = \mu_2)$. Hence $E = 1$ implies $Q \neq Q(t)$

(Q is constant) and it can be shown for the front position σ^i in the r,t-space in a layer with permeability k_0^i that $\sigma_i(t) = \sqrt{r_w^2 - \dfrac{2k_0^i \Delta p t}{\mu_1 \phi \ln(R/r_w)}}$ and hence $\dfrac{\sigma^1}{\sigma^2} \to \sqrt{\dfrac{k_0^1}{k_0^2}}$ as $t \to \infty$ ($t >> \dfrac{r_w^2 \mu_1 \phi \ln(R/r_w)}{2k_0^i \Delta p}$). To determine I when $E > 1$, we split the time into three intervals.

$0 < t \leq T$: During this interval viscous fluid is injected and we notice from the preceding subsection that there is a stable shock travelling with speed $Q(t)$ in the x,t-plane. Hence combining equation (3.8) with

$$S_1(x,t) = \begin{cases} 1, & x < s(t) \\ \\ 0, & x > s(t), \end{cases}$$

yields

$$I = \frac{\phi}{2} \left\{ \left[\ln(r_w^2 + 2\tilde{x}/\phi) \right]_0^{s(t)} + \frac{1}{E} \left[\ln(r_w^2 + 2\tilde{x}/\phi) \right]_{s(t)}^{L} \right\}. \tag{3.9}$$

Since for $0 < t \leq T$ we have $s(t) = \int_0^t Q(\chi) d\chi$, above equation combined with (3.8) gives an ordinary differential equation (ODE) in time with $s(t)$ to be determined. This ODE can be solved using analytical methods. Note that $s(t)$ is in the x,t-space, if $\sigma(t)$ is the front position in the r,t-space, then $\sigma(t) = (r_w^2 + 2s(t)/\phi)^{1/2}$.

$T < t \leq \tau$: During this interval water is injected and fingering takes place. Now the saturation $S_1(x,t)$ is given by

$$S_1(x,t) = \begin{cases} 0, & x \in \left[0, \frac{1}{E} \int_T^t Q(\chi) d\chi \right), \\ \\ \dfrac{\sqrt{\frac{E \int_T^t Q(\chi) d\chi}{x}} - E}{1 - E}, & x \in \left[\dfrac{1}{E} \displaystyle\int_T^t Q(\chi) d\chi, E \int_T^t Q(\chi) d\chi \right), \\ \\ 1, & x \in \left[E \int_T^t Q(\chi) d\chi, s(t) \right), \\ \\ 0, & x \geq s(t), \end{cases}$$

with $s(t) = \int_0^t Q(\chi) d\chi$.

Using above saturation relation the integral I can be computed using straightforward

integration, yielding

$$
\begin{aligned}
I &= \frac{\phi}{2E}\left[\ln(r_w^2+2\tilde{x}/\phi)\right]_0^{\frac{s(t)-s(T)}{E}} + \\
&+\frac{1}{\sqrt{E(s(t)-s(T))}}\left[\sqrt{\phi\tilde{x}}-\frac{r_w\phi^{3/2}\arctan(\frac{\sqrt{2\tilde{x}/\phi}}{r_w})}{\sqrt{2}}\right]_{\frac{s(t)-s(T)}{E}}^{E(s(t)-s(T))} + \\
&+\frac{\phi}{2}\left[\ln(r_w^2+2\tilde{x}/\phi)\right]_{E(s(t)-s(T))}^{s(t)}+\frac{\phi}{2E}\left[\ln(r_w^2+2\tilde{x}/\phi)\right]_{s(t)}^{L} \qquad (3.10)
\end{aligned}
$$

Above relation can be substituted into equation (3.8) to obtain an ODE for $s(t)$. However, due to the complexity of the relation we use a numerical time (Runge-Kutta) integration method to solve the ODE. We use the co-ordinate transformation $\sigma(t)=\left(r_w^2+2s(t)/\phi\right)^{1/2}$ to get the position of the front in the r,t-space.

$t>\tau$: During this interval still water is injected. However, this interval differs from preceding interval since the fingering zone overtook the shock, i.e. $E(s(t)-s(T))>s(t)$ for $t>\tau$. For this case the saturation profile is given by:

$$
S_1(x,t)=\begin{cases} 0, & x\in\left[0,\frac{1}{E}\int_T^t Q(\chi)d\chi\right), \\ \dfrac{\sqrt{\frac{E\int_T^t Q(\chi)d\chi}{x}}-E}{1-E}, & x\in\left[\dfrac{1}{E}\displaystyle\int_T^t Q(\chi)d\chi, s(t)\right], \\ 0, & x\geq s(t), \end{cases}
$$

The shock position $s(t)$ is given by

$$
s(t)=\left(\sqrt{s(\tau)}+\sqrt{\frac{1}{E}}\left\{\left[\int_T^t Q(\chi)d\chi\right]^{\frac{1}{2}}-\left[\int_T^\tau Q(\chi)d\chi\right]^{\frac{1}{2}}\right\}\right)^2. \qquad (3.11)
$$

The integral I is now given by

$$
\begin{aligned}
I &= \frac{\phi}{2E}\left[\ln(r_w^2+2\tilde{x}/\phi)\right]_0^{\frac{\int_T^t Q(\chi)d\chi}{E}} + \\
&+\frac{1}{\sqrt{E(s(t)-s(T))}}\left[\sqrt{\phi\tilde{x}}-\frac{r_w\phi^{3/2}\arctan(\frac{\sqrt{2\tilde{x}/\phi}}{r_w})}{\sqrt{2}}\right]_{\frac{\int_T^t Q(\chi)d\chi}{E}}^{s(t)} + \\
&+\frac{\phi}{2E}\left[\ln(r_w^2+2\tilde{x}/\phi)\right]_{s(t)}^{L} \qquad (3.12)
\end{aligned}
$$

This relation can be substituted in equation (3.8) to yield an ODE for $s(t)$ in time. We use the co-ordinate transformation $\sigma(t)=\left(r_w^2+2s(t)/\phi\right)^{1/2}$ to get the position of the front

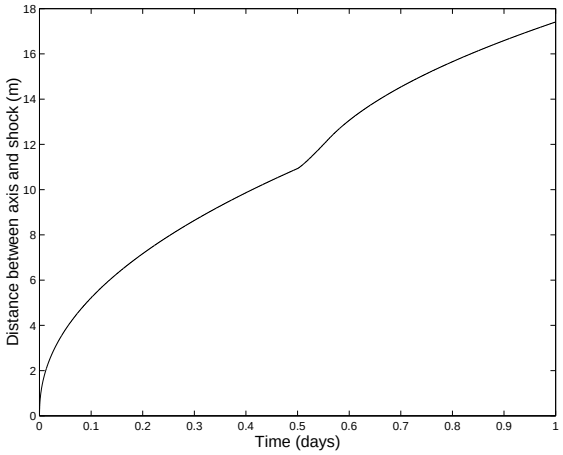

Figure 3: The propagation of the shock position as a function of time.

in the r, t-space. Combining obtained ODE with equation (3.11) we solve the obtained system using a Runge-Kutta time integration method. As an example we show in Figure 3 the shock propagation as a function of time for axial symmetry. In above example we use $\mu_1 = 1mPas$, $\Delta p = 10^7 Pa$ and $k_0 = 10^{-12}m^2$. It can be seen that the shock accellerates at $t > T$. However, for $t > \tau$ the shock velocity decreases.

4. Results

This section deals with a comparison between the analytical method as described in Section 3 and a numerical method. The numerical method is based on a Finite Difference discretisation of the equations. To minimise numerical diffusion near shock fronts, we use a higher order (flux-limiter) scheme. For the time discretisation we use the "theta-scheme". The presently used numerical scheme is standard. For more background we refer to [6], [4], [3], [2].

Figure 4 shows a numerical calculation corresponding to the same data as in Figure 4. One can see that the numerical results do not agree badly with those obtained from the analytical results. The numerical and analytical method predict approximately the same front velocity. Profiles from the numerical method are smoother due to numerical diffusion (see Figure 5). Thereby profiles from the numerical method exhibit a point of inflection near $x = x_L(t) = \frac{\mu_2}{\mu_1}Q(t - T)$. For larger times the solutions start to differ more significantly.

Subsequently we show an example from a technological application. We inject the viscous glycerol with volumetric flow $0.33\,l/s$ during two days. The viscosity of glycerol is $1000\,mPas$. The thickness of the reservoir and the well radius are respectively $5m$ and $0.1m$. The corresponding velocity is then $1 \cdot 10^{-4}m/s$. The porosity is 0.3. After these two days, we inject the much less viscous water phase $\mu = 1mPas$. Profiles at different times are shown in Figure 6. The calculations are based on the explicit solution from Section 3. Note that we transformed the solution back into cylindrical co-ordinates using

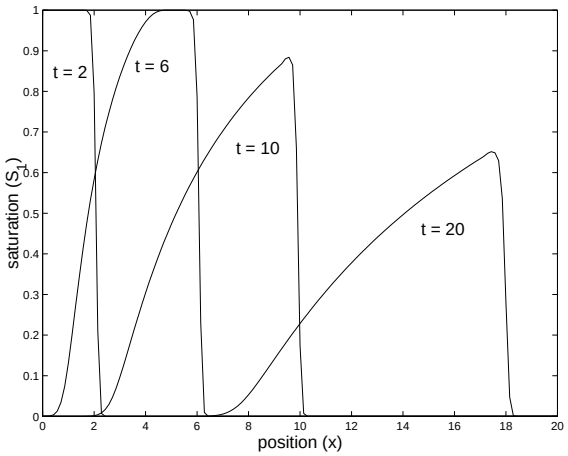

Figure 4: Saturation profiles at different times computed using the numerical method. Input data are similar to Figure 2.

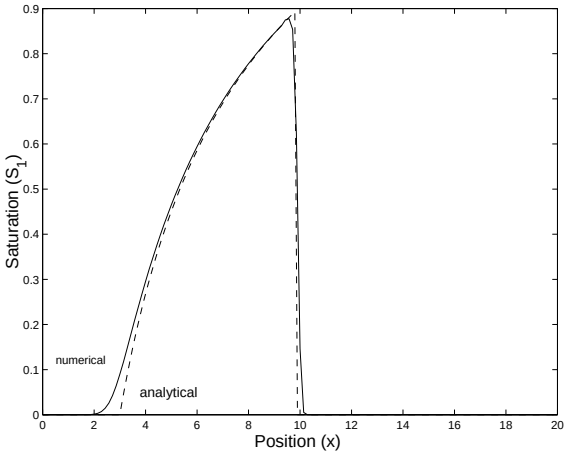

Figure 5: Saturation profiles for the same time ($t = 10$) and conditions for the numerical (solid curve) and analytical solution (dashed curve).

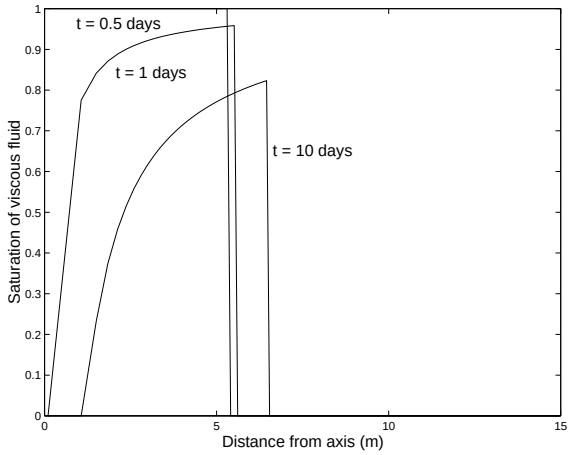

Figure 6: Saturation profiles for different times in a technological well. Input data are given in the text.

$r = \sqrt{r_w^2 + 2x/\phi}$, viz. Section 3. One can see that the front delays significantly for $t > T$. In Figure 7 we plot the pressure drop over the first 15 meters in the reservoir as a function of time for the same set of parameters as in Figure 6. During the injection of viscous glycerol the pressure increases linearly ($t < T$). For $t > T$ (i.e. injection of water) gives a non-linear behaviour due to presence of a fingering zone (rarefaction). The pressure has been computed using equation (3.6).

Now we give some examples of constant pressure condition. We did the calculations for different permeabilities. We show the shock position as a function of time in Figure 8. We entered the same data as for Figure 6, except for the pressure drop, Δp, for which we used $10^7 Pa$ and the viscocity of the preflush fluid $\mu_1 = 500 mPa\,s$. We entered $T = 0.5 days$. It can be seen in Figure 8 that the kink is more pronounced for high permeabilities. In Figure 9 we show the propagation of the front for different porosities. Clearly for lower porosity the shock speed is high. Figure 10 shows the influence of the viscosity of the preflush fluid on the shock movement. It can be seen clearly that for a less viscous preflush fluid the shock speed increases. Moreover, as the viscosity of the preflush fluid tends to the water viscosity, the behaviour of the shock position converges towards the case of a one phase flow.

We show the influence of the time, T, during which we inject the viscous fluid in Figure 11. It can be seen that for a technological situation already for 1.5 hour of injection a considerable distance (1.25 m) can be treated.

Finally we show the gel penetration depth as a function of time after several different preflush treatments. We consider a reservoir with permeability $k_0 = 10^{-12} m^2$. The pressure drop over the reservoir is $\Delta p = 10^7 Pa$. We plot the gel penetration depth x_L^i in layer i as a function of gelation time $(t - T)$ for different viscosity ratios, $E = \frac{\mu_1}{\mu_2}$, for the layers with

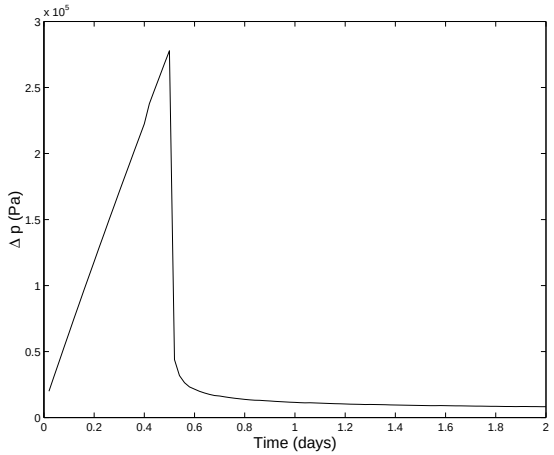

Figure 7: The pressure-drop in the reservoir over 15 meters from the axis as a function of time in days. Input data are similar to those in Figure 6

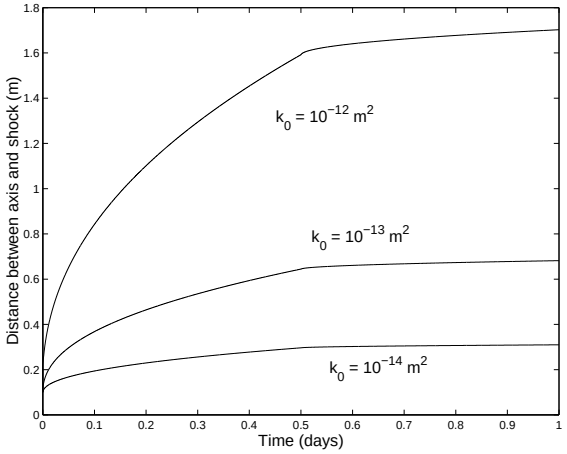

Figure 8: The shock position as a function of time for different permeabilities.

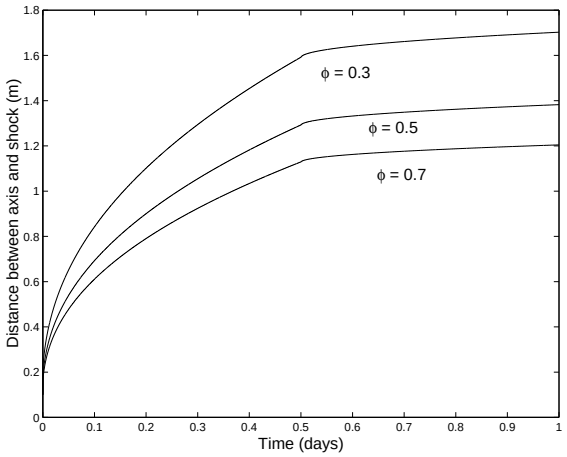

Figure 9: The shock position as a function of time for different porosities.

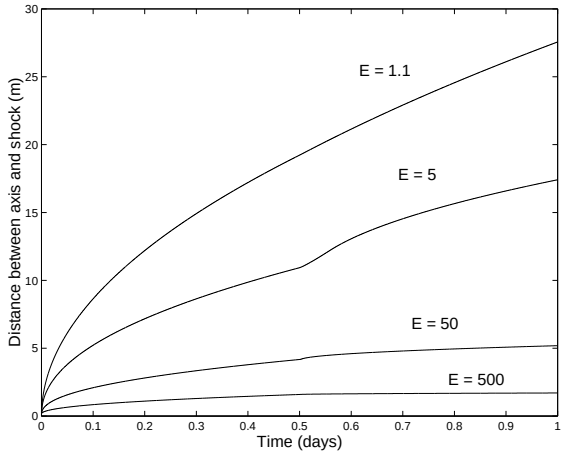

Figure 10: The shock position as a function of time for different viscosity ratios.

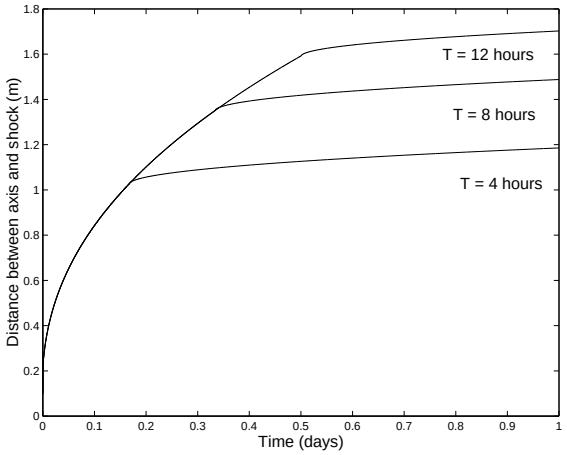

Figure 11: The shock position as a function of time for different preflush times.

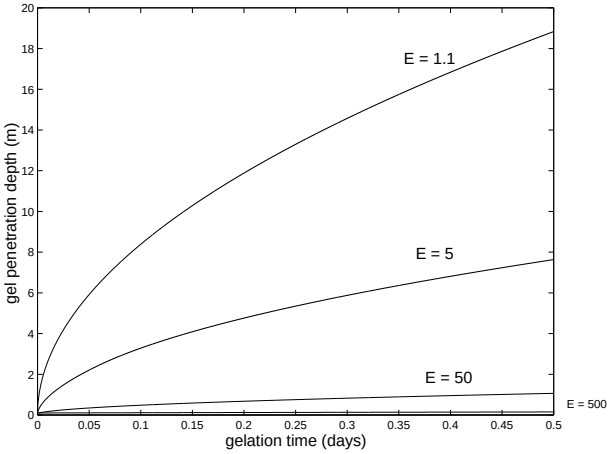

Figure 12: The gel penetration depth as a function of time for $k_0 = 10^{-12}m^2$ after half a day of preflush agent injection.

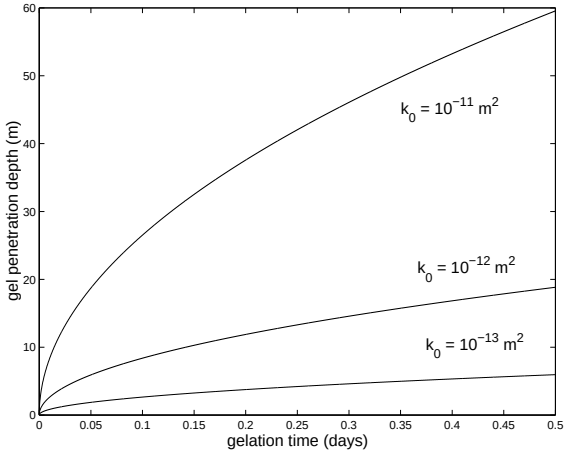

Figure 13: The gel penetration depth as a function of time for $E = 1.1$ after half a day of preflush agent injection.

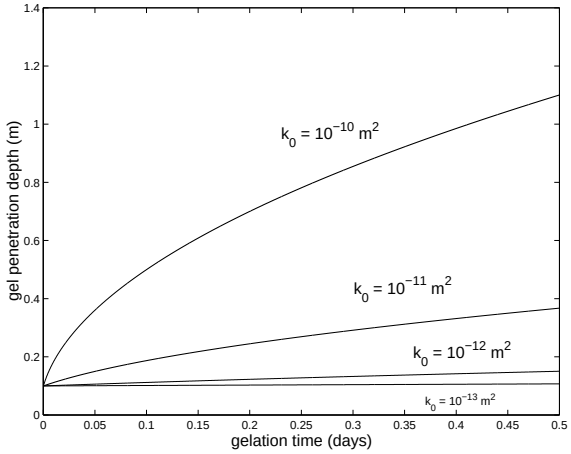

Figure 14: The gel penetration depth as a function of time for $E = 500$ after half a day of preflush agent injection.

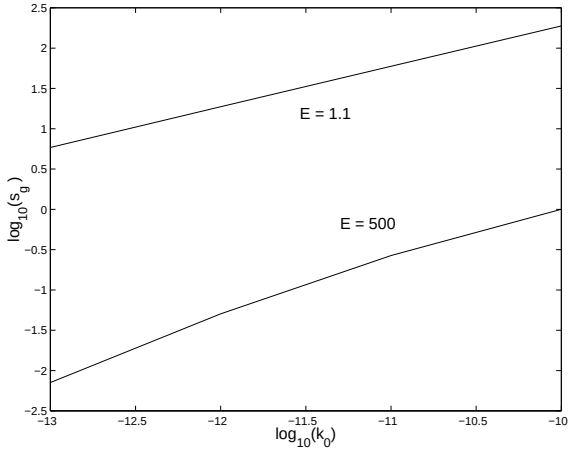

Figure 15: The logarithm of the penetration depth as a function of the logarithm of the pemeability for $E = 1.1$ and $E = 500$ after half a day of preflush injection.

permeability $k_0 = 10^{-12}m^2$ in Figure 12. It is clear from Figure 12 that the gel penetration depth decreases drastically as the viscosity ratio increases. Figure 13 displays the gel penetration depth for different permeabilities. All curves correspond to $E = 1.1$. Figure 14 shows the gel penetration depth for different permeabilities but for $E = 500$. For $k_0^1 > k_0^2$ it can be seen that $x_L^1/x_L^2 > (k_0^1/k_0^2)^{1/2}$ and $x_L^1/x_L^2 \to (k_0^1/k_0^2)^{1/2} = \sqrt{10}$ as $E \to 1$. For the illustration we plot the logarithm of the penetration depth as a function of the logarithm of the permeability in Figure 14. The curves correspond to $E = 1.1$ and $E = 500$. It can be seen in Figure 15 that the curve for $E = 1.1$ is a straigth line with slope $1/2$ and that the curve for $E = 500$ is concave. Its slope converges to $1/2$. From above we conclude that after preflush treatment the gel penetration depth in the low permeability layer decreases as the preflush fluid is more viscous. This observation agrees with numerical and experimental results of Stavland [8].

5. Conclusions

For the case of fully miscible fluids the preflush treatment can be modelled using explicit expressions. Profiles exhibit a viscous fingering zone between non-viscous and viscous fluids, whereas shocks persist as sharp interfaces between viscous and non-viscous fluids. For the case of constant pressure conditions a semi-explicit relation can be found for the position of the shock and the gel penetration depth. Application to a multi-layer reservoir shows that viscous preflush is an efficient treatment to divert polymer-gel flow from low permeability layers. High permeability layers can then be gel-treated efficiently. The model can be used for planar, cylindrical and spherical geometries.

Acknowledgement: This work was funded by the European Union (Welgel project) and by the Welgel industrial consortsium (BGplc, GDF, Halliburton, Norsk Conoco, Petrobras, Shell, SNF-Floerger, Statoil, Tarim Oilfield, Texaco and Total).

References

1. S.M.P. Blom. *Relative permeability to near-miscible fluids.* Thesis. Delft University Press, Delft University of Technology, 1999.
2. A. Harten. High resolution schemes for hyperbolic conservation laws. *Journal of computational physics*, 49:357, 1983.
3. W. Hundsdorfer and R.A. Trompert. Method of lines and direct discretisation: a comparison for linear advection. *Journal of Applied Numerical Analysis*, 13:469–490, 1994.
4. Willem Hundsdorfer. Trapezoidal and midpoint splittings for initial-boundary value problems. *Mathematics of Computation*, 67, 223:1047–1062, 1998.
5. E.J. Koval. A method for predicting the performance of unstable miscible displacement in heterogeneous media. *SPE Reprint Series*, 8, 1963.
6. Randall J. LeVeque. *Numerical methods for conservation laws.* 2. Birkhäuser Verlag, Zürich, 1992.
7. J. Smoller. *Shock waves and reaction-diffusion equations.* 1. Springer, New York, 1983.
8. Arne Stavland. Private communication. 1999.